BOREAL ENVIRONMENT RESEARCH 29: 131–148
ISSN 1797-2469 (online)

Helsinki 11 June 2024

The influence of dissolved organic matter composition on microbial degradation and carbon dioxide production in pristine subarctic rivers

Taija Saarela[1)*], Xudan Zhu[2)], Helena Jäntti[1)], Mizue Ohashi[3)], Jun'ichiro Ide[4)], Henri Siljanen[1)], Aake Pesonen[1)], Heidi Aaltonen[5)], Anne Ojala[6)], Hiroshi Nishimura[7)], Timo Kekäläinen[8)], Janne Jänis[8)], Frank Berninger[2)] and Jukka Pumpanen[1)]

[1)] *Department of Environmental and Biological Sciences, University of Eastern Finland, Kuopio, FI-70210, Finland*
[2)] *Department of Environmental and Biological Sciences, University of Eastern Finland, Joensuu, FI-80101, Finland*
[3)] *School of Human Science and Environment, University of Hyogo, Hyogo, 670-0092, Japan*
[4)] *Department of Applied Chemistry and Bioscience, Chitose Institute of Science and Technology, Chitose, 066-8655, Japan*
[5)] *Department of Agricultural Sciences, University of Helsinki, Helsinki, FI-00014, Finland*
[6)] *Natural Resources Institute Finland (Luke), Helsinki, FI-00790, Finland*
[7)] *Research Institute for Sustainable Humanosphere, Kyoto University, Kyoto, 606-8501, Japan*
[8)] *Department of Chemistry, University of Eastern Finland, Joensuu, FI-80101, Finland*
**corresponding author's e-mail: taija.saarela@uef.fi*

Received 21 Jun. 2023, final version received 30 Oct. 2023, accepted 9 Nov. 2023

Saarela T., Zhu X., Jäntti H., Ohashi M., Ide J., Siljanen H., Pesonen A., Aaltonen H., Ojala A., Nishimura H., Kekäläinen T., Jänis J., Berninger F. & Pumpanen J. 2024: The influence of dissolved organic matter composition on microbial degradation and carbon dioxide production in pristine subarctic rivers. *Boreal Env. Res.* 29: 131–148.

Dissolved organic matter (DOM) degradation in freshwaters plays an important role in the global carbon cycle, yet there is limited understanding of how the origin and composition of DOM regulate the production of riverine greenhouse gases. We investigated the molecular composition of DOM using Fourier transform ion cyclotron resonance mass spectrometry (FT-ICR MS) and measured the potential carbon dioxide (CO_2) production in pristine subarctic rivers of Finnish Lapland. During 21-day incubations, dissolved organic carbon (DOC) was effectively mineralized into CO_2 in the clearwater river associated with mineral soils. The high degradability of mineral soil-derived DOM was supported by a high presence of aliphatic and peptide-like compounds. Significantly lower CO_2 production per DOC was observed in the brown-water river, likely due to a large number of less biodegradable, vascular plant-derived compounds from surrounding peatlands. These findings highlight the significance of biolabile molecular compounds in the DOM degradation dynamics of subarctic catchments.

Editor in charge of this article: Örjan Östman

Introduction

The lateral transport of dissolved organic carbon (DOC) and nitrogen (DON) from catchments to freshwaters via surface flow or groundwater inputs is a crucial link between terrestrial and aquatic ecosystems (Battin *et al.* 2009). In a changing climate, northern freshwaters are exposed to increasing terrestrial dissolved organic matter (DOM) load due to changes in precipitation, air temperature and vegetation cover as well as due to reduced sulphur (S) deposition (Sarkkola *et al.* 2009, Couture *et al.* 2012, Pumpanen *et al.* 2014, Finstad *et al.* 2016, Monteith *et al.* 2023). The increases in the export of DOM have the potential to significantly accelerate aquatic CO_2 emissions across northern latitudes (Lapierre *et al.* 2013, Berggren and del Giorgio 2015). Similarly to lakes that are supersaturated with dissolved C gases due to terrestrial DOM inputs (Cole *et al.* 2007), recent studies have reported streams and rivers to be net sources of carbon dioxide (CO_2) and methane (CH_4) to the atmosphere (Aufdenkampe *et al.* 2011, Butman and Raymond 2011, Huotari *et al.* 2013, Rocher-Ros *et al.* 2019).

Small streams and rivers together with their riparian zones are hotspots of biogeochemical activity (McClain *et al.* 2003, Catalán *et al.* 2016) and play an important role in the global carbon cycle (Cole *et al.* 2007). Small fluvial systems as processors of DOM are particularly important in the northern landscape characterized by a high density of small streams and rivers that connect the numerous lakes and wetlands (Ågren *et al.* 2007). Recently, the molecular composition of DOM has gained increasing attention as a controller of DOM degradation (Kellerman *et al.* 2015, Mostovaya *et al.* 2017, Hawkes *et al.* 2018, Wologo *et al.* 2021). However, to our knowledge, there have been very few studies addressing the influence of molecular composition on mineralization of DOC to CO_2 (Hodgins *et al.* 2014, Valle *et al.* 2018).

DOM degradation in freshwaters depends on the combination of extrinsic (e.g., temperature, nutrient and oxygen availability, photochemical reactions, and bacterial community composition) and intrinsic factors (i.e., chemical properties of DOM) (Tranvik and Bertilsson 2001, Bastviken *et al.* 2004, Vähätalo and Wetzel 2008, Koehler *et al.* 2012, Catalán *et al.* 2021). DOM consists of a wide range of dissolved organic molecules, and it is among the most complex molecular mixtures known (Zark and Dittmar 2018). Recent developments of DOM characterization using Fourier transform ion cyclotron resonance mass spectrometry (FT-ICR MS) enable measurements of DOM molecular composition by identifying thousands of individual molecular formulas for a single sample (e.g., Hockaday *et al.* 2009). In recent years, FT-ICR MS has been used to identify the molecular composition of DOM in a variety of aquatic systems, including rivers (Rogers *et al.* 2021, Behnke *et al.* 2021), lakes (Kellerman *et al.* 2015, Mostovaya *et al.* 2017) and groundwater (McDonough *et al.* 2022). In aquatic ecosystems, the sources of DOM are typically categorized into allochthonous (terrestrially derived) and autochthonous (algal- and macrophyte-derived) sources (Stedmon *et al.* 2007). Autochthonous DOM is associated with lower molecular weight and higher bioavailability compared to allochthonous DOM (Chen and Wangersky 1996).

Hydrological conditions and catchment characteristics (e.g., soil type, vegetation, and land use) have a strong influence on DOM biogeochemistry in headwaters (Ågren *et al.* 2007, Spencer *et al.* 2008, Battin *et al.* 2009, Kothwala *et al.* 2015, Catalán *et al.* 2016). Northern high-latitude rivers are associated with seasonal fluctuations in hydrology (e.g., an intense runoff during the spring freshet and baseflow periods during the summer and winter), and these fluctuations largely control the export and composition of riverine DOM (Olefeldt *et al.* 2013, Kothwala *et al.* 2015). In subarctic ecosystems, the catchment-scale DOM export and composition are closely connected to the area covered by peatlands and the contribution of groundwater (Olefeldt *et al.* 2013). Peatland-derived DOM in freshwaters tends to have higher concentrations and aromatic content (i.e., lower bioavailability) compared to DOM derived from other terrestrial sources (Ågren *et al.* 2008, Olefeldt *et al.* 2013). Northern peatlands and forest soils are known to represent a major C reservoir (Gorham 1991, Tarnocai *et al.* 2009), and in peat-dominated catchments, the terrestrial production and fluvial export of DOM might be even more sensitive to climatic changes than in mineral soil catchments (Monteith *et al.* 2015).

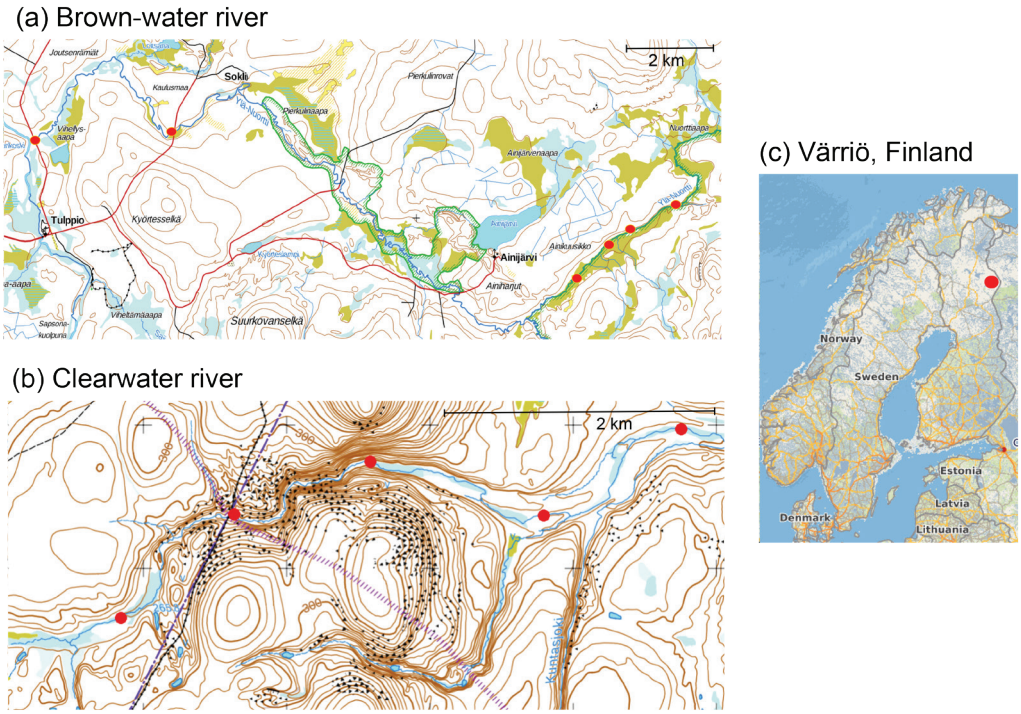

Fig. 1. (**a**) Brown-water river (river Yli-Nuortti); (**b**) Clearwater river (river Kotkakurunoja); and (**c**) the study area in Värriö Strict Nature Reserve (67°44´16´´N, 29°38´58´´E) in Finnish Lapland. Red dots represent the sampling locations. Map from National Land Survey of Finland, Paituli open access data base, open data CC-BY-4.0 license, available online: http://www.csc.fi/paituli.

Here, we investigate how the quantity and composition of DOM influence its microbial degradability and CO_2 production in subarctic rivers. We aimed to: 1) gain a more comprehensive understanding on the composition of riverine DOM at a molecular level; 2) determine how DOM microbial degradability and relative abundance of bacteria differ between the brown-water and clearwater river; and 3) investigate how these factors regulate the potential CO_2 production in the rivers. We hypothesized that DOM in the brown-water river has lower degradability than DOM in the clearwater river because the water originated from peatlands contains recalcitrant humic-like substances. We also hypothesized that DOM degradation is dependent on terrestrial plant-derived compounds during spring, while the role of autochthonous sources (e.g., macrophyte-derived DOM) is more pronounced during autumn.

Material and methods

Site description

Samples were collected from a subarctic coniferous forest located in Värriö Strict Nature Reserve (67°44´16´´N, 29°38´58´´E) in Finnish Lapland close to Värriö Subarctic Research Station (University of Helsinki) (Fig. 1c). The most dominant tree species in the region include Scots pine (*Pinus sylvestris* L.), Norway spruce (*Picea abies* ssp. *obovata*) and downy birch (*Betula pubescens* ssp. *pubescens*). The soils in the study area are haplic podzols with sand tills (FAO 1990). The climate is subcontinental with no underlying permafrost. The average annual precipitation and air temperature in the study area are 592 mm (Korhonen and Haavalammi 2012) and –1°C (Susiluoto *et al.* 2008), respectively. The length of the period of snow cover is 200–225 days, while the length of the growing season is 105–120 days (Pohjonen *et al.* 2008).

Experimental design

Sampling was carried out on two occasions (June 11–13 and October 8–10, 2018) to study the effect of the molecular composition of riverine DOM on microbial degradation and CO_2 production with 21-day incubation studies. The samples were collected from two rivers that differ in catchment characteristics (e.g., vegetation and soil type). Both rivers drain to Barents Sea. The brown-water river (Yli-Nuortti, Fig. 1a) is surrounded by pristine open mires with ~20% catchment peatland coverage. In the brown-water river catchment, the ground vegetation consists of dwarf shrubs (*Betula nana* L., *Salix glauca* L.), flowering plants (*Geranium sylvaticum* L.), graminoids, and mosses (*Sphagnum* L.). The clearwater river (Kotkakurunoja, Fig. 1b) flows from a steep gorge and is surrounded by mineral soils (< 1% catchment peatland coverage). The ground vegetation in the clearwater river catchment consists of dwarf shrubs (e.g., *Vaccinium myrtillus* L., *Vaccinium vitis idaea* L. and *Empetrum nigrum* L.), lichens (*Cladina* (Nyl.)) and mosses (e.g. *Polytrichum* sp. and *Pleurozium schreberi* (Brid.) Mitt.).

Water discharge was determined based on the continuous water depth measurements carried out by pressure sensors measuring the hydrostatic pressure (Levelogger, Solinst, Georgetown, Canada) at the bottom of the river which was corrected by barometric pressure measurements (Barologger, Solinst, Georgetown, Canada). The water depth measurements were converted to flow rates using channel cross-section, water depth and manual flow rate measurements (Flow Tracker Handheld ADV, SonTek, CA, USA) conducted at sampling locations. Between June and October 2018, the discharge varied from 0.99 to 1.01 $m^3\ s^{-1}$ in the brown-water river and from 0.10 to 0.12 $m^3\ s^{-1}$ in the clearwater river (Fig. S1 in the Supplementary Information).

Two liters of water were collected from six locations of the brown-water river and five locations of the clearwater river (Fig. 1a, b) to pre-combusted (450°C, 3 h) brown glass bottles that had been washed with 0.01 M nitric acid (HNO_3) and rinsed with acetone (C_3H_6O) and ultra-pure water (Milli-Q®). After water sampling, surface sediment from one sampling location of each river was collected for the inoculum of the incubation experiment. Immediately after transporting the samples from the field to the research station, water samples were filtered through the filtration assembly with pre-combusted (450°C, 3 h) glass microfiber filters with a nominal pore size of 0.7 µm (Whatman GF/F Glass Microfiber Filters, GE Healthcare Bio-Sciences, Marlborough, MA, USA). The samples were stored at ~0 °C by submerging them in a stream close to the research station for 2–4 days until further processing.

In the laboratory, surface sediment samples from both rivers were centrifuged to separate the particulate matter from the water, and 10 ml of the separated fluid was then added to 1 l of river water (1:100) as a microbial inoculum to stimulate the microbial activity in the incubation experiment. Thereafter, 300 ml of each sample with the inoculum from the respective river was transferred into a 500 ml glass bottle in three replicates. Furthermore, one replicate of each water sample without the inoculum and three replicates of Milli-Q water mixed with the inoculum from each river, as well as three replicates of Milli-Q water as a control, were included in the incubation (Fig. S2 in the Supplementary Information). Replicates with the inoculum were used to determine the potential production of CO_2. Because no significant difference in the potential CO_2 production was observed between the replicates with and without the inoculum, replicates without the inoculum were used to investigate the composition of DOM to avoid the possible disturbance resulted from the inoculum on the interpretation of results.

In the beginning of the incubation, 60 ml of water from each incubation bottle was taken to measure the concentrations of DOC and total nitrogen (TN), as well as wavelength specific UV-absorbance at 254 nm ($SUVA_{254}$). In addition, 60 ml of water from the bottles without the inoculum was taken to measure the DOM molecular composition with FT-ICR MS. Thereafter, the bottles were transferred outside to aerate the samples with ambient air for 15 minutes. Close to each incubation bottle, 25 ml of ambient air was taken for a background sample using 60 ml BD Plastipak™ syringes equipped with a BD Connecta 3-way stopcock valve (Becton, Dick-

inson and Company, NJ, USA), and the sample was injected with a hypodermic needle to airtight pre-evacuated 12 ml Exetainer® vials (Labco Ltd., Lampeter, Ceredigion, UK). Immediately after that, the incubation bottles were closed with Butyl Stopper and Aluminum screw caps and stored at +10°C in the dark for 24 hours, after which they were allowed to stabilize at room temperature (+21°C) and shaken vigorously for 3 minutes. 25 ml of sample from the gas phase was then taken through Butyl Stopper via a syringe and a needle and injected into a pre-evacuated Exetainer. After that, the bottles were opened, and 60 ml of water from the bottles with the inoculum was taken to measure $SUVA_{254}$ and the concentrations of DOC and TN in the water.

After the first 24 hours of the experiment, the same procedure was repeated three times for the replicates with the inoculum (2, 6 and 20 days from the beginning of the experiment) (Fig. S2 in the Supplementary Information). After 20 days from the beginning of the experiment, the procedure was also repeated for the replicates without the inoculum. Between the samplings, the incubation bottles were covered with loose aluminum foil on top of the bottle and stored at +10°C in the dark. The bottles were carefully inverted for aeration every 2–3 days between samplings.

DOC and TN analyses

The samples for DOC and TN analyses were stored frozen (–18°C) until further analysis. The concentrations of DOC and TN were determined with a standard method (SFS-EN 1484) using Shimadzu TOC-V_{CPH} (Shimadzu Corp., Kyoto, Japan). The biodegradable fraction of DOC (%BDOC) was assessed by determining the change in DOC concentration between the end of incubation (21 d) and the average initial concentration among replicates (0 d) (Catalán *et al.* 2021).

$SUVA_{254}$

Absorbance measurements were conducted at 254 nm using a 0.01 m quartz cuvette with Shimadzu UV-2401 (Shimadzu Co., Kyoto, Japan). Wavelength-specific UV-absorbance at 254 nm ($SUVA_{254}$), an indicator of DOM aromaticity, was calculated as the absorbance divided by DOC concentration (Weishaar *et al.* 2003).

The concentrations of CO_2

The CO_2 concentrations were measured using Agilent 7890B Gas Chromatograph (Agilent Technologies, Palo Alto, CA, USA) equipped with Gilson liquid handler GX271 autosampler (Gilson Inc., Middleton, WI, USA). The concentrations of CO_2 (the gas phase concentration after 24 hours minus the background ambient concentration) were calculated based on a one-point calibration with standard gas (AGA, Lidingö, Sweden), using Henry's Law and the appropriate temperature relationships (see Supplementary Methods for full details) (Stumm and Morgan 1981).

For the calculation of cumulative CO_2 production over the 21 days incubation experiment, CO_2 production rates (μmol l^{-1} d^{-1}) measured during the four 24 h gas samplings were determined. Cumulative sums of CO_2 production rates between each consecutive measurement were calculated for the entire duration of the incubation experiment by linear interpolation. To estimate the CO_2 production in relation to DOC content, the CO_2 production per DOC was calculated by dividing the CO_2 production rate (μmol l^{-1} d^{-1}) by the DOC concentration (μmol l^{-1}) in each incubation bottle at each time point. Thereafter, the cumulative sums of CO_2 production rates per DOC (CO_2/DOC ratios) between each consecutive measurement were calculated.

FT-ICR MS analysis

The molecular composition of DOM was analyzed from the samples without the inoculum before and after 21 days incubation using electrospray ionization (ESI) coupled to ultrahigh-resolution Fourier transform ion cyclotron resonance mass spectrometry (FT-ICR MS). Samples filtered through glass microfiber filters with a

nominal pore size of 0.7 µm (Whatman GF/F Glass Microfiber Filters) were prepared using the solid phase extraction (SPE) cartridge (Bond Elut® PPL SPE cartridges, Agilent, CA, USA) to remove inorganic salts (Kim *et al.* 2003, Dittmar *et al.* 2008). The samples were diluted with deionized water and methanol to yield a final sample composition of 50/50 (v/v) of water to methanol. The samples were injected into the FT-ICR MS (solariX 7.0T, Bruker Daltonics Inc., MA, USA) using a syringe pump. All spectra were externally and internally calibrated. The samples were analyzed three times per sample, and the peak list of mass-to-charge ratio (m/z) shared among the three analytical replicates was extracted. The molecular formula calculator (Molecular Formula Calculator ver. 1.0; ©NHMFL, 1998) was used to assign an expected molecular formula for each m/z value with a mass accuracy ≤ 0.5 ppm. The m/z values in the range of 150–500 were inserted into the molecular formula calculator. Since high errors can be associated with the assignments containing S and P (Mostovaya *et al.* 2017), these formulae were excluded from further analysis. A detailed description for ESI coupled to FT-ICR MS is presented in the Supplementary Methods.

The modified aromaticity index (AI_{mod}), a descriptor of the degree of aromaticity, was calculated as $AI_{mod} = [1 + C - ½O - ½(N + H)] / (C - ½O - N)$ (modified by Mostovaya *et al.* 2017 based on Koch and Dittmar 2006), where C, H, O, and N refer to a number of respective atoms per molecule. Molecular formulae were classified using AI_{mod} and oxygen-to-carbon (O/C) and hydrogen-to-carbon (H/C) ratios as follows: polyphenolics ($0.5 < AI_{mod} \leq 0.66$); condensed aromatics ($AI_{mod} > 0.66$); highly unsaturated and phenolics (HUPs; $AI_{mod} \leq 0.5$, $H/C < 1.5$, $O/C \leq 0.9$); aliphatic ($1.5 \leq H/C \leq 2.0$, $O/C \leq 0.9$ and $N = 0$); sugar-like ($O/C > 0.9$); and peptide-like compounds ($1.5 \leq H/C \leq 2.0$, and $N > 0$) (Behnke *et al.* 2021).

16S qPCR analysis

The number of bacteria in the water samples was analyzed by using 16S qPCR. The glass microfiber filters with a nominal pore size of 0.7 µm (Whatman GF/F Glass Microfiber Filters) used in the filtration of river water samples ($n = 6$ in the brown-water river and $n = 5$ in the clearwater river) were stored frozen at –18°C until further treatment. The filters were transferred to BeadBeater tubes with a sterilized spoon and homogenized with BeadBeater (BioSpec Products Inc., Bartlesville, OK, USA). BeadBeater lysis buffer was added to the tubes to store the sample material. Clean Whatman GF/F Glass Microfiber Filters were used as a control and treated similarly with samples. For DNA extraction, homogenized filters were transferred into a pre-cooled Lysing tube E (MP Biomedicals, USA) with a sterilized spoon. For a detailed description of DNA extraction protocol, see Siljanen *et al.* (2019). The 16S rRNA gene in water DNA extracts was PCR-amplified using F338-forward and R518-reverse primers. Reactions were carried out using 16S qPCR X1 Mastermix (Table S2 in the Supplementary Information). For detailed steps in the 16S rRNA protocol, see Table S3 in the Supplementary Information. It must be acknowledged that the number of bacteria used to compare the relative abundances between the river water samples is an approximation based on bacteria larger than 0.7 µm. The analysis did not include small microbes due to the use of the glass microfiber filter with a 0.7 µm nominal pore size.

Statistical analyses

To test for differences between rivers and sampling occasions in the cumulative CO_2 production, CO_2/DOC ratios, %BDOC, the number of 16S rRNA gene copies, DOC and TN concentrations and $SUVA_{254}$ (0 and 21 days), we applied an analysis of variance (ANOVA), coupled with Tukey's HSD post-hoc test (*aov* and *TukeyHSD* functions in R). Furthermore, to test for differences between rivers and sampling occasions in the molecular composition of DOM (i.e., m/z ratio, H/C and O/C ratios, and AI_{mod} values of assigned molecular formulas), the ANOVA coupled with Tukey's HSD post-hoc test was applied. In all cases, variables were tested for normality using a Shapiro–Wilk test (*shapiro.test* function in R). Log transformation was con-

ducted when the variables violated assumptions of normality ($SUVA_{254}$ and the number of 16S rRNA gene copies).

Multiple linear regression analyses were used to identify which variables (DOC and TN concentrations, $SUVA_{254}$, %BDOC, and the number of molecular formulas in van Krevelen diagram-derived classification groups) best explained the differences in the CO_2 production, i.e., the cumulative CO_2 production and CO_2/DOC ratio (cumulative sums of CO_2 production rates divided by the DOC concentration in each bottle between each consecutive measurement). Variables with high (> 5.0) variance inflation factors (VIF) were excluded from the models to remove multicollinearity. Best models were selected according to the lowest value of AICc index (Akaike information criterion). The models were calculated as:

$$CO_2 = DOC_0 + DOC_{21} + SUVA_0 + Peptide_0 + Condensed_0 \quad , \quad (1)$$

$$CO_2 / DOC = DOC_{21} + TN_{21} + Aliphatics_0 + Peptide_0 \quad , \quad (2)$$

where CO_2 is the cumulative CO_2 production (µmol l^{-1}), CO_2 / DOC is the cumulative CO_2 production per DOC concentration, DOC_0 and DOC_{21} are the concentration of DOC (µmol l^{-1}) before and after the incubation, $SUVA_0$ is $SUVA_{254}$ (mg l^{-1} m^{-1}) before the incubation, TN_{21} is the concentration of TN (µmol l^{-1}) after the incubation, and $Peptide_0$, $Condensed_0$ and $Aliphatics_0$ refer to the number of aliphatic, peptide-like and condensed aromatic compounds before the incubation. All statistical analyses were performed using R (ver. 3.6.2; R Core Team 2020) in RStudio (RStudio Team 2020).

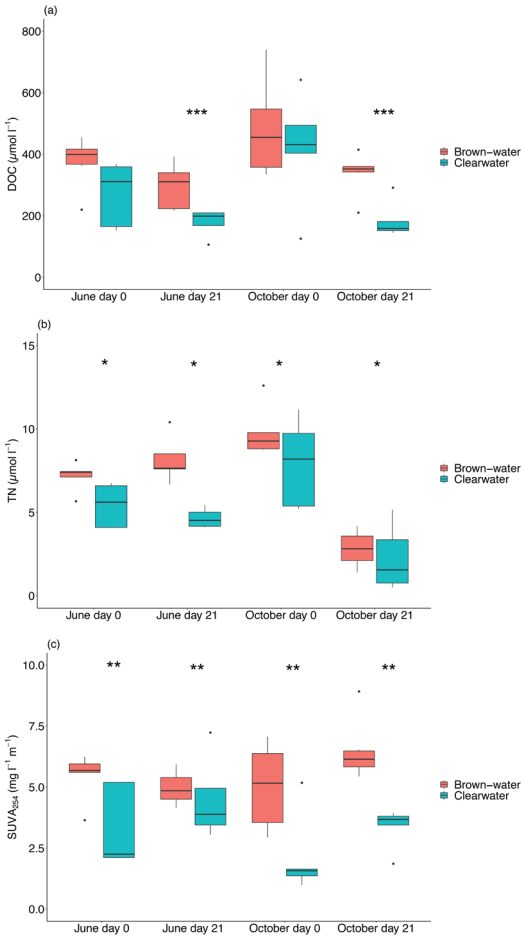

Fig. 2. The concentrations of (**a**) DOC (µmol l^{-1}); (**b**) TN (µmol l^{-1}); and (**c**) $SUVA_{254}$ (mg l^{-1} m^{-1}) over the incubation period (days 0 and 21) in June and October. Boxplots show the median (horizontal line), upper and lower quartile, as well as the smallest and largest value (n = 6 in the brown-water river and n = 5 in the clearwater river). Asterisks indicate significant differences between the brown-water and clearwater river. Level of significance: *** significant at $p < 0.001$, ** significant at $p < 0.01$, and * significant at $p < 0.05$.

Results

DOC and TN concentrations and $SUVA_{254}$

The DOC concentration was significantly higher in the brown-water river (range 217–392 µmol l^{-1} in June and 210–415 µmol l^{-1} in October) than in the clearwater river (106–210 µmol l^{-1} in June and 144–291 µmol l^{-1} in October) after 21 days of incubation (two-way ANOVA $F_{1,17} = 22.77$, $p < 0.001$), while at the beginning of incubation, the differences in the DOC concentration were smaller than the variability (Fig. 2a). The decrease in the DOC concentration over the incubation was statistically significant only in the clearwater river during October (one-way ANOVA $F_{7,33} = 4.67$, $p = 0.04$; Fig. 2a).

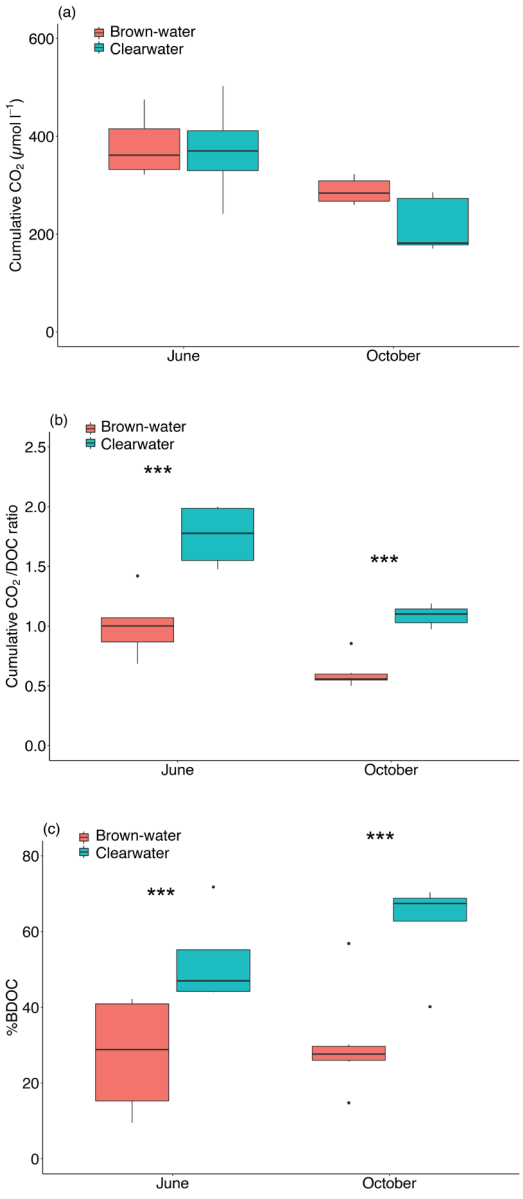

Fig. 3. (**a**) Cumulative CO_2 production; (**b**) cumulative CO_2/DOC ratio (the CO2 production per DOC); and (**c**) the proportion of BDOC (%) over the incubation period (21 days) in June and October. Boxplots show the median (horizontal line), upper and lower quartile, as well as the smallest and largest value (n = 6 in the brown-water river and n = 5 in the clearwater river). Asterisks indicate significant differences between the brown-water and clearwater river. Level of significance: *** significant at $p < 0.001$, ** significant at $p < 0.01$, and * significant at $p < 0.05$.

At the beginning of incubation, the concentration of TN was significantly higher in the brown-water river (5.7–8.1 μmol l^{-1} in June and 8.8–12.6 μmol l^{-1} in October) than in the clearwater river (4.1–6.7 μmol l^{-1} in June and 5.2–11.2 μmol l^{-1} in October) (two-way ANOVA $F_{1,18} = 5.11$, $p = 0.04$; Fig. 2b). Furthermore, the brown-water river had significantly higher TN concentrations (5.5–10.4 μmol l^{-1} in June and 1.4–4.2 μmol l^{-1} in October) compared to the clearwater river (4.0–5.4 μmol l^{-1} in June and 0.5–5.1 μmol l^{-1} in October) after the incubation (two-way ANOVA $F_{1,19} = 7.89$, $p = 0.01$; Fig. 2b). In both rivers, the concentration of TN decreased over the incubation during October (one-way ANOVA $F_{7,35} = 9.05$, $p < 0.001$ in the brown-water river and $p = 0.005$ in the clearwater river; Fig. 2b), while the decreases in TN were not statistically significant during June (Fig. 2b).

$SUVA_{254}$ was higher in the brown-water river both before (3.6–6.2 mg l^{-1} m^{-1} in June and 2.9–7.1 mg l^{-1} m^{-1} in October) and after the incubation (4.2–10.9 mg l^{-1} m^{-1} in June and 5.4–8.9 mg l^{-1} m^{-1} in October) (two-way ANOVA $F_{1,15} = 15.69$, $p = 0.001$ and $F_{1,15} = 13.99$, $p = 0.002$, respectively; Fig. 2c). In the clearwater river, $SUVA_{254}$ values ranged between 2.1–5.2 mg l^{-1} m^{-1} (June) and 1.0–5.2 mg l^{-1} m^{-1} (October) before the incubation, and 3.0–7.2 mg l^{-1} m^{-1} (June) and 1.9–3.9 mg l^{-1} m^{-1} (October) after the incubation (Fig. 2c).

Microbial degradation of DOM

The cumulative CO_2 production was not significantly different between the clearwater and brown-water rivers. The cumulative CO_2 production decreased from June (range 242–502 μmol l^{-1} in the clearwater river and 321–475 μmol l^{-1} in the brown-water river) to October (171–285 μmol l^{-1} in the clearwater river and 260–322 μmol l^{-1} in the brown-water river) (two-way ANOVA $F_{1,18} = 18.25$, $p < 0.001$; Fig. 3a). The cumulative ratios of CO_2/DOC, reflecting the degradation of DOC into CO_2, were higher in the clearwater river (1.5–2.0 in June and 1.0–1.2 in October) than in the brown-water river (0.7–1.4 in June and 0.5–0.9 in October) (two-way ANOVA $F_{1,18} = 46.41$, $p < 0.001$; Fig. 3b).

The cumulative CO_2/DOC ratio decreased in both rivers from June to October (two-way ANOVA $F_{1,18} = 29.57$, $p < 0.001$; Fig. 3b). The biodegradable proportion of DOC (%BDOC) was significantly higher in the clearwater river (43–71% in June and 40–70% in October) than in the brown-water river (9–42% in June and 14–57% in October) (two-way ANOVA $F_{1,16} = 20.94$, $p < 0.001$; Fig. 3c).

The molecular composition of DOM

The molecular composition of river water samples was determined using FT-ICR MS (Table S4 in the Supplementary Information). Number of molecular formulas assigned to each compound class varied between the rivers and seasons (Figs. 4 and 5). In both rivers, the molecular composition of DOM was dominated by highly unsaturated and phenolic compounds (HUPs). HUPs accounted for over 50% of total assigned molecular formulas in both rivers (Fig. 5b, d). The percentage (%) of molecular formulas above the molecular lability boundary (MLB) at H/C ≥ 1.5 (i.e., aliphatic, peptide-like and sugar-like molecular formulas) ranged from 22% to 30% in the clearwater river and from 18% to 22% in the brown-water river (Table S4 in the Supplementary Information). While the percentage of formulas assigned to aliphatics was similar in both rivers during June (13–15%; Fig. 5b), the clearwater river had a clearly higher percentage of aliphatic molecular formulas in October (24% in the clearwater river and 12% in the brown-water river; Fig. 5d). In addition, the percentage of formulas assigned to peptide-like compounds was higher in the clearwater river (9%) than in the brown-water river (4%) during June (Fig. 5b). Both in June and October, the brown-water river was associated with a higher percentage of condensed aromatics (11–12%) and polyphenolics (13–15%) compared to the clearwater river (Fig. 5b, d).

In both rivers, the molecular compound classes changed moderately over the incubation. In the clearwater river, the changes in DOM molecular composition were most evident in formulas assigned to aliphatics, which decreased by 6% in October (Fig. 5d). In June, the percentage of molecular formulas assigned to HUPs decreased by 7% in the brown-water river after 21 days of incubation (Fig. 5b). Furthermore, in October, the percentage of condensed aromatics decreased by 3% and polyphenols by 2% in the brown-water river (Fig. 5d).

Bacterial abundance in rivers

The number of bacterial 16S rRNA gene copies quantified from October water samples varied between 4.91×10^3 l^{-1} and 5.78×10^6 l^{-1} in the clearwater river (Fig. 6). In the brown-water river, the concentration of bacterial 16S rRNA genes ranged from 1.74×10^4 l^{-1} to 6.10×10^5 l^{-1}. The number of bacterial 16S rRNA gene copies did not differ significantly between the rivers due to the large variation within sampling locations.

Relationships between microbial degradation and molecular composition of DOM

The variables influencing potential CO_2 production were assessed in two multiple linear regression models (Table S5 in the Supplementary Information). Model 1 (Eq. 1) explained a statistically significant and substantial proportion of variance in the cumulative CO_2 production ($r^2 = 0.75$, $F_{5,12} = 7.07$, $p = 0.003$, adjusted $r^2 = 0.64$). The concentration of DOC, $SUVA_{254}$, and the number of peptide-like compounds and condensed aromatics at the beginning of incubation had significant positive relationships with the cumulative CO_2 production (intercept $\beta = 0.35$, SE = 0.16 and $p = 0.047$, $\beta = 39.58$, SE = 9.99 and $p = 0.002$, $\beta = 5.49$, SE = 1.55 and $p = 0.004$, and $\beta = 1.86$, SE = 0.79 and $p = 0.04$, respectively), while there was a negative relationship between the cumulative CO_2 production and DOC concentration after the incubation ($\beta = -0.61$, SE = 0.24 and $p = 0.02$). Model 2 (Eq. 2) explained a statistically significant and substantial proportion of variance in the cumulative ratios of CO_2/DOC ($r^2 = 0.76$, $F_{4,13} = 10.51$, $p < 0.001$, adjusted $r^2 = 0.69$). There was a significant positive relationship between CO_2/DOC ratio and the number of peptide-like compounds at the beginning of incubation ($\beta = 0.02$, SE = 0.01 and $p = 0.007$).

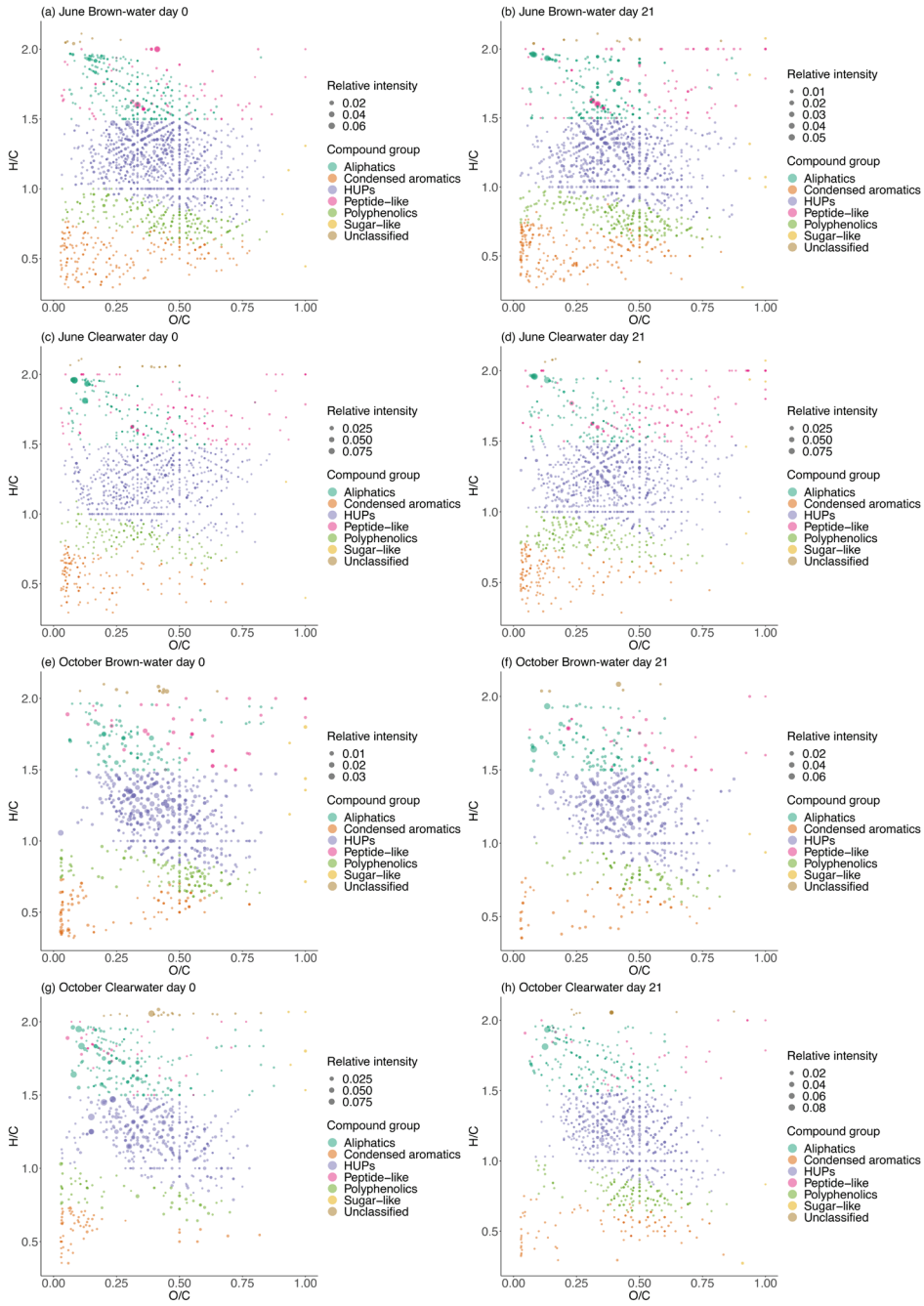

Fig. 4. Molecular element ratios (van Krevelen diagrams) from the FT-ICR MS analysis of river water samples in June: (**a**) Brown-water river before incubation; (**b**) Brown-water river after 21-day incubation; (**c**) Clearwater river before incubation; and (**d**) Clearwater river after 21-day incubation; and in October (**e**) Brown-water river before incubation; (**f**) Brown-water river after 21-day incubation; (**g**) Clearwater river before incubation; and (**h**) Clearwater river after 21-day incubation. Different colors represent compound groups assigned using AI_{mod} and oxygen-to-carbon (O/C) and hydrogen-to-carbon (H/C) ratios as follows: polyphenolics ($0.5 < AI_{mod} \leq 0.66$); condensed aromatics ($AI_{mod} > 0.66$); highly unsaturated and phenolics (HUPs; $AI_{mod} \leq 0.5$, $H/C < 1.5$, $O/C \leq 0.9$); aliphatic ($1.5 \leq H/C \leq 2.0$, $O/C \leq 0.9$ and $N = 0$); sugar-like ($O/C > 0.9$); and peptide-like compounds ($1.5 \leq H/C \leq 2.0$, and $N > 0$). Different sizes of bubbles represent peak intensities normalized to the sum of all signal intensities in each sample.

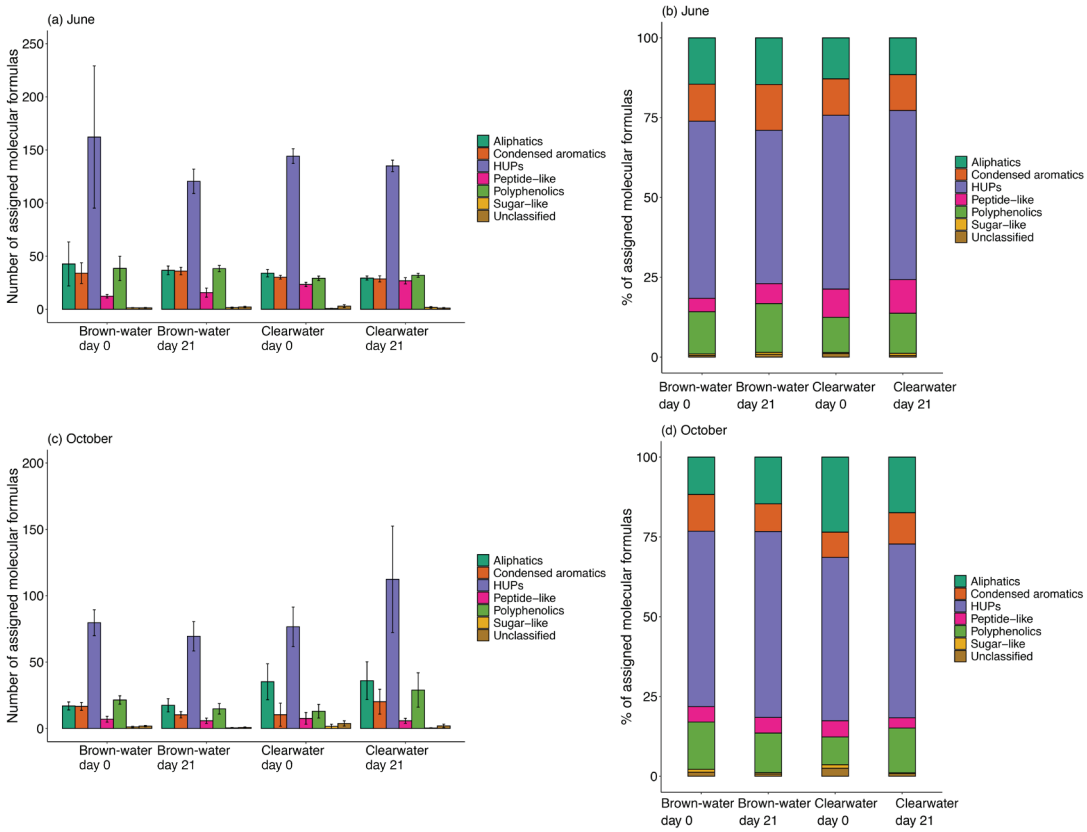

Fig. 5. Comparison of average values of the number of m/z peaks (± standard error) from the FT-ICR MS analysis in each compound group in (**a**) June and (**c**) October, and percentages of molecular formulas assigned to each compound group (based on the number of m/z peaks) in (**b**) June and (**d**) October. Compound groups were assigned using AI_{mod} and oxygen-to-carbon (O/C) and hydrogen-to-carbon (H/C) ratios as follows: polyphenolics ($0.5 < AI_{mod} \leq 0.66$); condensed aromatics ($AI_{mod} > 0.66$); highly unsaturated and phenolics (HUPs; $AI_{mod} \leq 0.5$, $H/C < 1.5$, $O/C \leq 0.9$); aliphatic ($1.5 \leq H/C \leq 2.0$, $O/C \leq 0.9$ and $N = 0$); sugar-like ($O/C > 0.9$); and peptide-like compounds ($1.5 \leq H/C \leq 2.0$, and $N > 0$).

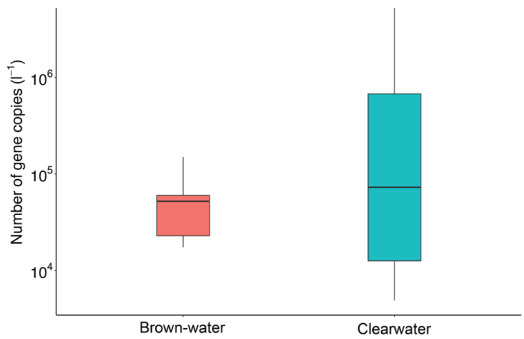

Fig. 6. (**a**) Abundance of bacterial communities estimated by quantifying the bacterial 16S rRNA gene copies (l^{-1}) in brown-water and clearwater river during October 2018. Boxplots show the median (horizontal line), upper and lower quartile, as well as the smallest and largest value ($n = 6$ in the brown-water river and $n = 5$ in the clearwater river).

Discussion

We conducted the combination of potential CO_2 production measurements and molecular-level characterization of DOM with water from two subarctic river ecosystems that represent contrasting types of catchment characteristics. The results demonstrate a higher mineralization of DOC into CO_2 in mineral soil-associated clearwater river during 21 days of incubation under controlled conditions. In contrast, significantly lower CO_2 production per DOC was observed in water from the brown-water river surrounded by peatlands (Fig. 3b). The higher microbial degradation of mineral soil-associated DOM, as indicated by CO_2/DOC, coincided with significantly lower aromaticity ($SUVA_{254}$) in the

clearwater river compared to the brown-water river (Fig. 2c). The degradation dynamics of mineral soil-associated DOM suggest the presence of more labile, easily biodegradable compounds in the DOM pool of the clearwater river (Kalbitz *et al.* 2003, Roth *et al.* 2019). Indeed, we found a high proportion of molecular formulas above the molecular lability boundary (MLB, H/C ≥ 1.5; D'Andrilli *et al.* 2015) in the clearwater river (22–30% of all assigned molecular formulas), including aliphatic and peptide-like compounds (Fig. 5). The abundance of these compounds has been associated with high bioavailability and microbial activity in fluvial systems (Behnke *et al.* 2022, Begum *et al.* 2023). The positive relationship between the cumulative CO_2 production per DOC and the number of peptide-like molecular formulas at the beginning of incubation further supports these observations.

Since molecular compounds with high H/C ratios are often derived from algal sources (Chen *et al.* 2016, Mostovaya *et al.* 2017, Liu *et al.* 2020), the aliphatic-rich signature in the clearwater river during October (24% of total assigned molecular formulas) could also indicate DOM of algal origin. Algal-derived DOM is associated with higher bioavailability compared to terrestrial or plant-derived DOM (Guillemette *et al.* 2013), and it supports a greater growth efficiency of bacteria (Kritzberg *et al.* 2005). In October, the decline in the percentage of aliphatics over the incubation (Fig. 5d) further implies that aliphatic compounds were important substrates for aquatic microbial metabolism in the clearwater river (Chróst and Gajewski 2006, Berggren *et al.* 2010, Spencer *et al.* 2015).

In the brown-water river, the lower CO_2 production per DOC under controlled conditions together with higher aromaticity (i.e., $SUVA_{254}$ values) indicate that the degradability of peatland-derived DOM was more limited compared to mineral soil-derived DOM (Figs. 2c and 3b). This observation is further supported by the significantly lower proportion of biodegradable DOC (BDOC%) in the brown-water river compared to the clearwater river (Fig. 3c). The limited degradability coincided with a large number of terrestrial and aromatic compounds in the DOM pool of the brown-water river (i.e., highly unsaturated and phenolic compounds, condensed aromatics and polyphenolics) (Figs. 4 and 5). These compounds are vascular plant-derived lignin compounds that most probably originated from surrounding peatlands (Spencer *et al.* 2008, Mostovaya *et al.* 2017, Behnke *et al.* 2021). The abundance of lignin compounds is typical of colored, peatland-derived DOM with high aromatic content (Ågren *et al.* 2008, Zark and Dittmar 2018). Lignin compounds tend to be degraded at a lower rate than other plant-derived compounds (e.g., cellulosic and non-cellulosic polysaccharides and proteins) (Martin *et al.* 1980).

During both spring and fall, the studied rivers were strongly dominated by highly unsaturated and phenolic compounds (HUPs), as is typical of DOM globally (Behnke *et al.* 2021, Rogers *et al.* 2021, Wologo *et al.* 2021, McDonough *et al.* 2022). HUPs have been attributed to vascular-plant derived lignin degradation products and chemically stable carboxylic-rich alicyclic molecules (CRAM) (Hertkorn *et al.* 2006, Roth *et al.* 2019). Interestingly, HUPs have been found to be more stable over time than compounds with higher aromatic content (i.e., condensed aromatics and polyphenolics) (Kellerman *et al.* 2015, Mostovaya *et al.* 2017).

While peatland-derived DOM was associated with limited degradability in our 21-day incubation experiments, DOM from different sources can become similarly bioavailable at timescales of months to years (Vähätalo and Wetzel 2008, Koehler *et al.* 2012). This is because compared to vascular plant-derived components of terrestrial origin, the degradation of more labile fractions of DOM (i.e., aliphatic and peptide-like compounds) mainly occurs on shorter timescales due to the rapid turnover of the low-molecular-weight compounds (Kalbitz *et al.* 2003). In contrast, highly unsaturated compounds, such as CRAMs, might accumulate in the water due to their resistance to rapid microbial degradation (Mostovaya *et al.* 2017, Wen *et al.* 2022). In both rivers, $SUVA_{254}$ values increased over the incubation, suggesting preferential microbial uptake of low-molecular-weight labile compounds and a relative increase in the aromaticity of DOM over the incubation (Drake *et al.* 2015, Raudina *et al.* 2022). On timescales longer than a month,

the compositional similarities between the rivers (e.g., the predominance of HUPs) could ultimately lead to diminished differences in DOM degradability. While the majority of DOM biodegradation is known to occur within 28 days from the beginning of the incubation (Vonk *et al.* 2015), a longer time step (e.g., several months) could be included in future incubation experiments to assess the relevance of slowly degrading DOM fractions on overall degradation potential of riverine DOM. It must be acknowledged, however, that DOM processing in these rivers is affected by a variety of physical and hydrological processes (e.g., transit times, radiation, and turbulence) that cannot be addressed by the incubation approaches. Also, while it is strongly recommended to conduct incubations at a stable temperature (Vonk *et al.* 2015), this approach cannot consider the temperature dependence of stream metabolism that has important implications for mineralization of DOC into CO_2 (Demars *et al.* 2011). Based on earlier studies (Jankowski *et al.* 2014), the temperature sensitivity of DOM processing might also differ between the studied rivers draining contrasting types of catchments with variation in geomorphic and chemical conditions. Furthermore, while the incubations were conducted in the dark, sunlight can play an important role in DOM processing of Arctic freshwaters (i.e., DOM photodegradation, Cory *et al.* 2014), resulting in the formation of labile molecular compounds available for subsequent microbial degradation (Moran and Zepp 1997). Since humic, shallow waters are typically rich in light-absorbing chromophoric DOM (CDOM) labile to photodegradation (Cory *et al.* 2014), the role of DOM photodegradation could be relevant in the brown-water river.

The results in the studied rivers showed higher CO_2 production per DOC during spring than later in the year (Fig. 3b). Although this study was only performed twice a year, the results agree with previous studies showing that the DOM exported during spring is younger and more labile than during other seasons (Neff *et al.* 2006, Raymond *et al.* 2007, Holmes *et al.* 2008). At the same time, the results also suggest that DOM exported during spring was highly aromatic (Figs. 2c and 5), which is similar to previous Arctic river studies showing the chemical paradox of spring freshet DOM being both biolabile and aromatic (Spencer *et al.* 2008, Behnke *et al.* 2021). The differences in DOM composition and biodegradability between spring and fall could be related to the dominant source of DOM shifting from surface runoff during the spring freshet to groundwater during base flow conditions (Guo and MacDonald 2006, Neff *et al.* 2006, Spencer *et al.* 2008). For example, Shen *et al.* (2015) found that groundwater DOM was associated with lower bioavailability and molecular weight compared to surface water, suggesting that DOM had undergone extensive microbial alteration in the groundwater. Furthermore, longer water residence times during base flow might also result in extensively processed DOM that is relatively resistant to microbial degradation (Wickland *et al.* 2007) and persistent in aquatic environments (Kellerman *et al.* 2015). On the other hand, the increased abundance of benthic macrophytes in both rivers during fall (observed by ocular perception) could also explain the transition toward DOM with lower biodegradability. It has been reported that some macrophyte species can release DOC from their roots to stimulate endomycorrhizal (Wigand *et al.* 1998) or microbial activity (Catalán *et al.* 2014) in the sediment, and that a significant fraction of the DOC produced by macrophytes can remain in the water as unreactive low-molecular-weight molecules (They *et al.* 2013). The variations in DOM microbial degradability during spring and fall thus suggest that the degradation of these complex DOM pools is not only regulated by their composition and concentrations but also by hydrologic controls on the export of DOM, as well as shifts between allochthonous and autochthonous sources of DOM.

Across northern landscapes, climate-induced terrestrial greening and changing hydrology are expected to accelerate the export of DOM from terrestrial to aquatic ecosystems (Bragazza *et al.* 2013, Finstad *et al.* 2016, Zhu *et al.* 2022, Tank *et al.* 2023). However, given the slower degradation potential of peatland-derived DOM compared to DOM from other sources (Fig. 3b), increased export of terrestrial plant-derived aromatic compounds may not lead to increased aquatic CO_2 flux potentials in northern peat-dominated catchments. Low-molecular-weight com-

pounds derived from mineral soil catchments are typically more mobile than high-molecular-weight aromatic compounds from peatlands (Kaiser *et al.* 2002), and they have a short turnover time in receiving waters, which allows continuous export of dissolved labile metabolites to aquatic ecosystems (Berggren *et al.* 2010). Our data revealed efficient mineralization of biolabile DOC into CO_2 in mineral soil-associated clearwater river during the incubation, highlighting the importance of aliphatic and peptide-like compounds in the DOM degradation dynamics of subarctic rivers. These findings underscore the relevance of mineral soil-associated clearwater systems for DOM processing in northern high-latitude catchments.

Conclusions

For the first time, we conducted the combination of molecular-level characterization of DOM and the potential CO_2 production measurements in two subarctic rivers located in the pristine areas of Finnish Lapland and draining to Barents Sea. The results showed efficient mineralization of DOC into CO_2 in mineral soil-associated clearwater river during the incubation. The high microbial degradation of mineral soil-associated DOM was supported by a high presence of aliphatic and peptide-like molecular compounds, providing evidence for microbial activity in the clearwater river. These results emphasize the importance of energy-rich, bioavailable DOM substrates and the role of clearwater systems in the DOM degradation dynamics of subarctic catchments. While northern freshwaters are exposed to high loads of DOM from surrounding peat soils, peatland-derived DOM in the brown-water river had lower degradability compared to DOM in the clearwater river. This was likely caused by a large number of less biodegradable, vascular plant-derived compounds in the DOM pool of the brown-water river. The slower degradation potential of peatland-derived DOM suggests that increasing export of terrestrial plant-derived compounds due to climate change may not necessarily stimulate aquatic CO_2 production in subarctic peatland catchments.

Acknowledgements: We thank Johanna Kerttula and Inga Paasisalo for help in field work and laboratory analyses. This research was funded by Doctoral Programme in Environmental Physics, Health and Biology, University of Eastern Finland; the Academy of Finland (275127, 307331, 326818, 323997); MEXT KAKENHI (20346689, JP15K16115, JP18K11623, JP19K22444, JP20KK0241 and JP22H02385); Japan Society for the Promotion of Science (JSBP120-209933, FY2018); Research Institute for Sustainable Humanosphere (RISH), Kyoto University; and joint funding by Olvi Foundation, Jenny and Antti Wihuri Foundation, and Saastamoinen Foundation (UEF Water).

Supplementary Information: The supplementary information related to this article is available online at: http://www.borenv.net/BER/archive/pdfs/ber29/ber29-xxx-xxx-supplement.pdf

References

Ågren A., Buffam I., Berggren M., Bishop K., Jansson M. & Laudon H. 2008. Dissolved organic carbon characteristics in boreal streams in a forest-wetland gradient during the transition between winter and summer. *Journal of Geophysical Research* 113: G03031.

Ågren A., Buffam I., Jansson M. & Laudon H. 2007. Importance of seasonality and small streams for the landscape regulation of dissolved organic carbon export: Seasonal and Landscape Regulation of DOC. *Journal of Geophysical Research: Biogeosciences* 112.

Aufdenkampe A.K., Mayorga E., Raymond P.A., Melack J.M., Doney S.C., Alin S.R., Aalto R.E. & Yoo K. 2011. Riverine coupling of biogeochemical cycles between land, oceans, and atmosphere. *Frontiers in Ecology and the Environment* 9: 53–60.

Bastviken D., Persson L., Odham G. & Tranvik L. 2004. Degradation of dissolved organic matter in oxic and anoxic lake water. *Limnology and Oceanography* 49: 109–116.

Battin T.J., Luyssaert S., Kaplan L.A., Aufdenkampe A.K., Richter A. & Tranvik L.J. 2009. The boundless carbon cycle. *Nature Geoscience* 2: 598–600.

Begum M.S., Park J.-H., Yang L., Shin K.H. & Hur J. 2023. Optical and molecular indices of dissolved organic matter for estimating biodegradability and resulting carbon dioxide production in inland waters: A review. *Water Research* 228: 119362.

Behnke M.I., McClelland J.W., Tank S.E., Kellerman A.M., Holmes R.M., Haghipour N., Eglinton T.I., Raymond P.A., Suslova A., Zhulidov A.V., Gurtovaya T., Zimov N., Zimov S., Mutter E.A., Amos E. & Spencer R.G.M. 2021. Pan-Arctic Riverine Dissolved Organic Matter: Synchronous Molecular Stability, Shifting Sources and Subsidies. *Global Biogeochemical Cycles* 35.

Berggren M. & del Giorgio P.A. 2015. Distinct patterns of microbial metabolism associated to riverine dissolved organic carbon of different source and quality. *Journal of Geophysical Research: Biogeosciences* 120: 989–999.

Berggren M., Ström L., Laudon H., Karlsson J., Jonsson A., Giesler R., Bergström A.-K. & Jansson M. 2010. Lake secondary production fueled by rapid transfer of low molecular weight organic carbon from terrestrial sources to aquatic consumers: Terrestrial LMWC and lake secondary production. *Ecology Letters* 13: 870–880.

Bragazza L., Parisod J., Buttler A. & Bardgett R.D. 2013. Biogeochemical plant–soil microbe feedback in response to climate warming in peatlands. *Nature Climate Change* 3: 273–277.

Butman D. & Raymond P.A. 2011. Significant efflux of carbon dioxide from streams and rivers in the United States. *Nature Geoscience* 4: 839–842.

Catalán N., Marcé R., Kothawala D.N. & Tranvik Lars.J. 2016. Organic carbon decomposition rates controlled by water retention time across inland waters. *Nature Geoscience* 9: 501–504.

Catalán N., Pastor A., Borrego C.M., Casas-Ruiz J.P., Hawkes J.A., Gutiérrez C., Schiller D. & Marcé R. 2021. The relevance of environment vs. composition on dissolved organic matter degradation in freshwaters. *Limnology and Oceanography* 66: 306–320.

Catalán, N., Obrador, B. & Pretus, J.L. 2014. Ecosystem processes drive dissolved organic matter quality in a highly dynamic water body. *Hydrobiologia* 728: 111–124.

Chen M., Kim S., Park J.-E., Kim H.S. & Hur J. 2016. Effects of dissolved organic matter (DOM) sources and nature of solid extraction sorbent on recoverable DOM composition: Implication into potential lability of different compound groups. *Analytical and Bioanalytical Chemistry* 408: 4809–4819.

Chen W. & Wangersky P.J. 1996. Rates of microbial degradation of dissolved organic carbon from phytoplankton cultures. *Journal of Plankton Research* 18: 1521–1533.

Chróst R.J. & Gajewski A.J. 2006. Microbial utilization of lipids in lake water. *FEMS Microbiology Ecology* 18: 45–50.

Cole J.J., Prairie Y.T., Caraco N.F., McDowell W.H., Tranvik L.J., Striegl R.G., Duarte C.M., Kortelainen P., Downing J.A., Middelburg J.J. & Melack J. 2007. Plumbing the Global Carbon Cycle: Integrating Inland Waters into the Terrestrial Carbon Budget. *Ecosystems* 10: 172–185.

Cory R.M., Ward C.P., Crump B.C. & Kling G.W. 2014. Sunlight controls water column processing of carbon in arctic fresh waters. *Science* 345: 925–928.

Couture S., Houle D. & Gagnon C. 2012. Increases of dissolved organic carbon in temperate and boreal lakes in Quebec, Canada. *Environmental Science and Pollution Research* 19: 361–371.

D'Andrilli J., Cooper W.T., Foreman C.M. & Marshall A.G. 2015. An ultrahigh-resolution mass spectrometry index to estimate natural organic matter lability. *Rapid Communications in Mass Spectrometry* 29: 2385–2401.

Demars B.O.L., Russell Manson J., Ólafsson J.S., Gíslason G.M., Gudmundsdóttir R., Woodward G., Reiss J., Pichler D.E., Rasmussen J.J. & Friberg N. 2011. Temperature and the metabolic balance of streams: Temperature and the metabolic balance of streams. *Freshwater Biology* 56: 1106–1121.

Dittmar T., Koch B., Hertkorn N. & Kattner G. 2008. A simple and efficient method for the solid-phase extraction of dissolved organic matter (SPE-DOM) from seawater: SPE-DOM from seawater. *Limnology and Oceanography: Methods* 6: 230–235.

Drake T.W., Wickland K.P., Spencer R.G.M., McKnight D.M. & Striegl R.G. 2015. Ancient low–molecular-weight organic acids in permafrost fuel rapid carbon dioxide production upon thaw. *Proceedings of the National Academy of Sciences* 112: 13946–13951.

Finstad A.G., Andersen T., Larsen S., Tominaga K., Blumentrath S., Wit H.A. de, Tømmervik H. & Hessen D.O. 2016. From greening to browning: Catchment vegetation development and reduced S-deposition promote organic carbon load on decadal time scales in Nordic lakes. *Scientific Reports* 6: 31944.

Gorham E. 1991. Northern Peatlands: Role in the Carbon Cycle and Probable Responses to Climatic Warming. *Ecological Applications* 1: 182–195.

Guillemette F., McCallister S.L. & Giorgio P.A. del. 2013. Differentiating the degradation dynamics of algal and terrestrial carbon within complex natural dissolved organic carbon in temperate lakes: DOC degradation dynamics in lakes. *Journal of Geophysical Research: Biogeosciences* 118: 963–973.

Guo L. & Macdonald R.W. 2006. Source and transport of terrigenous organic matter in the upper Yukon River: Evidence from isotope ($\delta^{13}C$, $\Delta^{14}C$, and $\delta^{15}N$) composition of dissolved, colloidal, and particulate phases: source and transport of organic matter. *Global Biogeochemical Cycles* 20.

Hawkes J.A., Radoman N., Bergquist J., Wallin M.B., Tranvik L.J. & Löfgren S. 2018. Regional diversity of complex dissolved organic matter across forested hemiboreal headwater streams. *Scientific Reports* 8: 16060.

Hertkorn N., Benner R., Frommberger M., Schmitt-Kopplin P., Witt M., Kaiser K., Kettrup A. & Hedges J.I. 2006. Characterization of a major refractory component of marine dissolved organic matter. *Geochimica et Cosmochimica Acta* 70: 2990–3010.

Hockaday W.C., Purcell J.M., Marshall A.G., Baldock J.A. & Hatcher P.G. 2009. Electrospray and photoionization mass spectrometry for the characterization of organic matter in natural waters: a qualitative assessment: Characterization of organic matter in natural waters. *Limnology and Oceanography: Methods* 7: 81–95.

Hodgkins S.B., Tfaily M.M., McCalley C.K., Logan T.A., Crill P.M., Saleska S.R., Rich V.I. & Chanton J.P. 2014. Changes in peat chemistry associated with permafrost thaw increase greenhouse gas production. *Proceedings of the National Academy of Sciences* 111: 5819–5824.

Holmes R.M., McClelland J.W., Raymond P.A., Frazer B.B., Peterson B.J. & Stieglitz M. 2008. Lability of DOC transported by Alaskan rivers to the Arctic Ocean. *Geophysical Research Letters* 35: L03402.

Huotari J., Haapanala S., Pumpanen J., Vesala T. & Ojala A. 2013. Efficient gas exchange between a boreal river and the atmosphere: efficient gas exchange of a large river. *Geophysical Research Letters* 40: 5683–5686.

Ide J., Ohashi M., Köster K., Berninger F., Miura I., Makita N., Yamase K., Palviainen M. & Pumpanen J. 2020a.

Molecular composition of soil dissolved organic matter in recently-burned and long-unburned boreal forests. *International Journal of Wildland Fire* 29: 541.

Jankowski K., Schindler D.E. & Lisi P.J. 2014. Temperature sensitivity of community respiration rates in streams is associated with watershed geomorphic features. *Ecology* 95: 2707–2714.

Kaiser K., Guggenberger G., Haumaier L. & Zech W. 2002. The composition of dissolved organic matter in forest soil solutions: changes induced by seasons and passage through the mineral soil. *Organic Geochemistry* 33: 307–318.

Kalbitz K., Schwesig D., Schmerwitz J., Kaiser K., Haumaier L., Glaser B., Ellerbrock R. & Leinweber P. 2003. Changes in properties of soil-derived dissolved organic matter induced by biodegradation. *Soil Biology and Biochemistry* 35: 1129–1142.

Kellerman A.M., Kothawala D.N., Dittmar T. & Tranvik L.J. 2015. Persistence of dissolved organic matter in lakes related to its molecular characteristics. *Nature Geoscience* 8: 454–457.

Kim S., Simpson A.J., Kujawinski E.B., Freitas M.A. & Hatcher P.G. 2003. High resolution electrospray ionization mass spectrometry and 2D solution NMR for the analysis of DOM extracted by C18 solid phase disk. *Organic Geochemistry* 34: 1325–1335.

Koch B.P. & Dittmar T. 2006. From mass to structure: an aromaticity index for high-resolution mass data of natural organic matter. *Rapid Communications in Mass Spectrometry* 20: 926–932.

Koehler B., Wachenfeldt E. von, Kothawala D. & Tranvik L.J. 2012. Reactivity continuum of dissolved organic carbon decomposition in lake water: reactivity continuum of lake DOC. *Journal of Geophysical Research: Biogeosciences* 117.

Korhonen J. & Haavanlammi E. 2012. Hydrologinen vuosikirja 2006–2010/Hydrological Yearbook 2006–2010. *Suomen ympäristökeskus* 8/2012.

Kothawala D.N., Ji X., Laudon H., Ågren A.M., Futter M.N., Köhler S.J. & Tranvik L.J. 2015. The relative influence of land cover, hydrology, and in-stream processing on the composition of dissolved organic matter in boreal streams. *Journal of Geophysical Research: Biogeosciences* 120: 1491–1505.

Kritzberg E., Cole J., Pace M. & Granéli W. 2005. Does autochthonous primary production drive variability in bacterial metabolism and growth efficiency in lakes dominated by terrestrial C inputs? *Aquatic Microbial Ecology* 38: 103–111.

Lapierre J.-F., Guillemette F., Berggren M. & Giorgio P.A. del. 2013. Increases in terrestrially derived carbon stimulate organic carbon processing and CO_2 emissions in boreal aquatic ecosystems. *Nature Communications* 4: 2972.

Liu S., He Z., Tang Z., Liu L., Hou J., Li T., Zhang Y., Shi Q., Giesy J.P. & Wu F. 2020. Linking the molecular composition of autochthonous dissolved organic matter to source identification for freshwater lake ecosystems by combination of optical spectroscopy and FT-ICR-MS analysis. *Science of The Total Environment* 703: 134764.

Martin J.P., Haider K. & Kassim G. 1980. Biodegradation and Stabilization after 2 Years of Specific Crop, Lignin, and Polysaccharide Carbons in Soils. *Soil Science Society of America Journal* 44: 1250–1255.

McClain M.E., Boyer E.W., Dent C.L., Gergel S.E., Grimm N.B., Groffman P.M., Hart S.C., Harvey J.W., Johnston C.A., Mayorga E., McDowell W.H. & Pinay G. 2003. Biogeochemical Hot Spots and Hot Moments at the Interface of Terrestrial and Aquatic Ecosystems. *Ecosystems* 6: 301–312.

McDonough L.K., Andersen M.S., Behnke M.I., Rutlidge H., Oudone P., Meredith K., O'Carroll D.M., Santos I.R., Marjo C.E., Spencer R.G.M., McKenna A.M. & Baker A. 2022. A new conceptual framework for the transformation of groundwater dissolved organic matter. *Nature Communications* 13: 2153.

Monteith D. T., Henrys P. A., Evans C. D., Malcolm I., Shilland E. M. & Pereira M. G. 2015. Spatial Controls on Dissolved Organic Carbon in Upland Waters Inferred from a Simple Statistical Model. *Biogeochemistry* 123 (3): 363–77.

Monteith D.T., Henrys P.A., Hruška J., De Wit H.A., Krám P., Moldan F., Posch M., Räike A., Stoddard J.L., Shilland E.M., Pereira M.G. & Evans C.D. 2023. Long-term rise in riverine dissolved organic carbon concentration is predicted by electrolyte solubility theory. *Science Advances* 9: eade3491.

Moran M.A. & Zepp R.G. 1997. Role of photoreactions in the formation of biologically labile compounds from dissolved organic matter. *Limnology and Oceanography* 42: 1307–1316.

Mostovaya A., Hawkes J.A., Dittmar T. & Tranvik L.J. 2017. Molecular Determinants of Dissolved Organic Matter Reactivity in Lake Water. *Frontiers in Earth Science* 5: 106.

Neff J.C., Finlay J.C., Zimov S.A., Davydov S.P., Carrasco J.J., Schuur E.A.G. & Davydova A.I. 2006. Seasonal changes in the age and structure of dissolved organic carbon in Siberian rivers and streams. *Geophysical Research Letters* 33: L23401.

Olefeldt D., Roulet N., Giesler R. & Persson A. 2013. Total waterborne carbon export and DOC composition from ten nested subarctic peatland catchments-importance of peatland cover, groundwater influence, and inter-annual variability of precipitation patterns: waterborne carbon export from subarctic catchments. *Hydrological Processes* 27: 2280–2294.

Pohjonen V., Mönkkönen P. & Hari P. 2008. Test of northern timber line. In P. H. L. K. (Ed.), *Boreal forest and climate change* (pp. 472-475). (Advances in global change research; Vol. 34). Springer.

Pumpanen J., Lindén A., Miettinen H., Kolari P., Ilvesniemi H., Mammarella I., Hari P., Nikinmaa E., Heinonsalo J., Bäck J., Ojala A., Berninger F. & Vesala T. 2014. Precipitation and net ecosystem exchange are the most important drivers of DOC flux in upland boreal catchments: Precipitation and NEE drive runoff DOC. *Journal of Geophysical Research: Biogeosciences* 119: 1861–1878.

Raudina T.V., Smirnov S.V., Lushchaeva I.V., Istigechev G.I., Kulizhskiy S.P., Golovatskaya E.A., Shirokova L.S.

& Pokrovsky O.S. 2022. Seasonal and Spatial Variations of Dissolved Organic Matter Biodegradation along the Aquatic Continuum in the Southern Taiga Bog Complex, Western Siberia. *Water* 14: 3969.

Raymond P.A., McClelland J.W., Holmes R.M., Zhulidov A.V., Mull K., Peterson B.J., Striegl R.G., Aiken G.R. & Gurtovaya T.Y. 2007. Flux and age of dissolved organic carbon exported to the Arctic Ocean: A carbon isotopic study of the five largest arctic rivers: arctic river DOC. *Global Biogeochemical Cycles* 21.

Rocher-Ros G., Sponseller R.A., Lidberg W., Mörth C. & Giesler R. 2019. Landscape process domains drive patterns of CO_2 evasion from river networks. *Limnology and Oceanography Letters* 4: 87–95.

Rogers J.A., Galy V., Kellerman A.M., Chanton J.P., Zimov N. & Spencer R.G.M. 2021. Limited Presence of Permafrost Dissolved Organic Matter in the Kolyma River, Siberia Revealed by Ramped Oxidation. *Journal of Geophysical Research: Biogeosciences* 126.

Roth V.-N., Lange M., Simon C., Hertkorn N., Bucher S., Goodall T., Griffiths R.I., Mellado-Vázquez P.G., Mommer L., Oram N.J., Weigelt A., Dittmar T. & Gleixner G. 2019. Persistence of dissolved organic matter explained by molecular changes during its passage through soil. *Nature Geoscience* 12: 755–761.

Sarkkola S., Koivusalo H., Laurén A., Kortelainen P., Mattsson T., Palviainen M., Piirainen S., Starr M. & Finér L. 2009. Trends in hydrometeorological conditions and stream water organic carbon in boreal forested catchments. *Science of The Total Environment* 408: 92–101.

Shen Y., Chapelle F.H., Strom E.W. & Benner R. 2015. Origins and bioavailability of dissolved organic matter in groundwater. *Biogeochemistry* 122: 61–78.

Siljanen H.M.P., Alves R.J.E., Ronkainen J.G., Lamprecht R.E., Bhattarai H.R., Bagnoud A., Marushchak M.E., Martikainen P.J., Schleper C. & Biasi C. 2019. Archaeal nitrification is a key driver of high nitrous oxide emissions from arctic peatlands. *Soil Biology and Biochemistry* 137: 107539.

Spencer R.G.M., Aiken G.R., Wickland K.P., Striegl R.G. & Hernes P.J. 2008. Seasonal and spatial variability in dissolved organic matter quantity and composition from the Yukon River basin, Alaska: Yukon River basin DOM dynamics. *Global Biogeochemical Cycles* 22.

Spencer R.G.M., Mann P.J., Dittmar T., Eglinton T.I., McIntyre C., Holmes R.M., Zimov N. & Stubbins A. 2015. Detecting the signature of permafrost thaw in Arctic rivers: signature of permafrost thaw in rivers. *Geophysical Research Letters* 42: 2830–2835.

Stedmon C.A., Thomas D.N., Granskog M., Kaartokallio H., Papadimitriou S. & Kuosa H. 2007. Characteristics of Dissolved Organic Matter in Baltic Coastal Sea Ice: Allochthonous or Autochthonous Origins? *Environmental Science & Technology* 41: 7273–7279.

Stumm W. & Morgan J.J. 1981. Aquatic Chemistry: An Introduction Emphasizing Chemical Equilibria in Natural Waters. 2nd Edition, John Wiley & Sons Ltd., New York.

Susiluoto S., Rasilo T., Pumpanen J. & Berninger F. 2008. Effects of Grazing on the Vegetation Structure and Carbon Dioxide Exchange of a Fennoscandian Fell Ecosystem. *Arctic, Antarctic, and Alpine Research* 40: 422–431.

Tank S.E., McClelland J.W., Spencer R.G.M., Shiklomanov A.I., Suslova A., Moatar F., Amon R.M.W., Cooper L.W., Elias G., Gordeev V.V., Guay C., Gurtovaya T.Yu., Kosmenko L.S., Mutter E.A., Peterson B.J., Peucker-Ehrenbrink B., Raymond P.A., Schuster P.F., Scott L., Staples R., Striegl R.G., Tretiakov M., Zhulidov A.V., Zimov N., Zimov S. & Holmes R.M. 2023. Recent trends in the chemistry of major northern rivers signal widespread Arctic change. *Nature Geoscience* 16: 789–796.

Tarnocai C., Canadell J.G., Schuur E.A.G., Kuhry P., Mazhitova G. & Zimov S. 2009. Soil organic carbon pools in the northern circumpolar permafrost region: soil organic carbon pools. *Global Biogeochemical Cycles* 23.

They N.H., Motta Marques D. da & Souza R.S. 2013. Lower Respiration in the Littoral Zone of a Subtropical Shallow Lake. *Frontiers in Microbiology* 3.

Tranvik L.J. & Bertilsson S. 2001. Contrasting effects of solar UV radiation on dissolved organic sources for bacterial growth. *Ecology Letters* 4: 458–463.

Vähätalo A.V. & Wetzel R.G. 2008. Long-term photochemical and microbial decomposition of wetland-derived dissolved organic matter with alteration of 13C:12C mass ratio. *Limnology and Oceanography* 53: 1387–1392.

Valle J., Gonsior M., Harir M., Enrich-Prast A., Schmitt-Kopplin P., Bastviken D., Conrad R. & Hertkorn N. 2018. Extensive processing of sediment pore water dissolved organic matter during anoxic incubation as observed by high-field mass spectrometry (FTICR-MS). *Water Research* 129: 252–263.

Vonk J.E., Tank S.E., Mann P.J., Spencer R.G.M., Treat C.C., Striegl R.G., Abbott B.W. & Wickland K.P. 2015. Biodegradability of dissolved organic carbon in permafrost soils and aquatic systems: a meta-analysis. *Biogeosciences* 12: 6915–6930.

Weishaar J.L., Aiken G.R., Bergamaschi B.A., Fram M.S., Fujii R. & Mopper K. 2003. Evaluation of Specific Ultraviolet Absorbance as an Indicator of the Chemical Composition and Reactivity of Dissolved Organic Carbon. *Environmental Science & Technology* 37: 4702–4708.

Wen Z., Shang Y., Song K., Liu G., Hou J., Lyu L., Tao H., Li S., He C., Shi Q. & He D. 2022. Composition of dissolved organic matter (DOM) in lakes responds to the trophic state and phytoplankton community succession. *Water Research* 224: 119073.

Wickland K.P., Neff J.C. & Aiken G.R. 2007. Dissolved Organic Carbon in Alaskan Boreal Forest: Sources, Chemical Characteristics, and Biodegradability. *Ecosystems* 10: 1323–1340.

Wigand C., Andersen F.O., Christensen K.K., Holmer M. & Jensen H.S. 1998. Endomycorrhizae of isoetids along a biogeochemical gradient. *Limnology and Oceanography* 43: 508–515.

Wologo E., Shakil S., Zolkos S., Textor S., Ewing S., Klassen J., Spencer R.G.M., Podgorski D.C., Tank S.E., Baker M.A., O'Donnell J.A., Wickland K.P., Foks S.S.W., Zar-

netske J.P., Lee-Cullin J., Liu F., Yang Y., Kortelainen P., Kolehmainen J., Dean J.F., Vonk J.E., Holmes R.M., Pinay G., Powell M.M., Howe J., Frei R.J., Bratsman S.P. & Abbott B.W. 2021. Stream Dissolved Organic Matter in Permafrost Regions Shows Surprising Compositional Similarities but Negative Priming and Nutrient Effects. *Global Biogeochemical Cycles* 35.

Zark M. & Dittmar T. 2018. Universal molecular structures in natural dissolved organic matter. *Nature Communications* 9: 3178.

Zhu X., Chen L., Pumpanen J., Ojala A., Zobitz J., Zhou X., Laudon H., Palviainen M., Neitola K. & Berninger F. 2022. The role of terrestrial productivity and hydrology in regulating aquatic dissolved organic carbon concentrations in boreal catchments. *Global Change Biology* 28: 2764–2778.